THE JOURNAL OF PHYSICAL CHEMISTRY C

Article

pubs.acs.org/JPCC

Insight Into the Effect of CuNi(111) and FeNi(111) Surface Structure and Second Metal Composition on Surface Carbon Elimination by O or OH: A Comparison Study with Ni(111) Surface

Riguang Zhang, Xiaoqiang Guo, Baojun Wang,* and Lixia Ling

Key Laboratory of Coal Science and Technology of Ministry of Education and Shanxi Province, Taiyuan University of Technology, Taiyuan 030024, Shanxi, P.R. China

Supporting Information

ABSTRACT: A density functional theory (DFT) calculation has been carried out to systematically investigate the mechanism of surface carbon elimination by O and OH on both the alloy FeNi(111) and CuNi(111) surfaces, including the homogeneous and the segregated surfaces, respectively; meanwhile, the obtained results are compared with those on the pure Ni(111) surface in order to probe into the effects of CuNi(111) and FeNi(111) surface structure and second metal composition on the performance of surface carbon elimination. Our results show that compared to the pure Ni(111) surface, the introduction of Fe into Ni increases the adsorption of O, OH, and C species, while it weakens the adsorption of CO and COH; the incorporation of Cu into Ni decreases the adsorption ability of C, O, OH, CO, and COH species. The mechanism of surface carbon elimination by O and OH shows that OH species is more effective for carbon elimination than O species on Ni(111), CuNi(111) surface and the segregated FeNi(111) surface; meanwhile, CuNi(111) and FeNi(111) surface structure and second metal composition have obvious effect on the performance of carbon elimination. Compared to Ni(111), FeNi(111) surface is not favorable for carbon elimination, while CuNi(111) surface is beneficial for carbon elimination, in which the Cu enriched surface is much more favorable than the 1:1 Cu surface and the pure Ni(111), indicating that the segregated CuNi(111) surface with Cu enrichment significantly accelerates carbon elimination. Moreover, the good linear relationship exists between the average adsorption energy of C + O or C + OH and the activation barrier of the C + O(OH) reaction. As a result, once carbon is formed on the segregated CuNi alloy surface with Cu enrichment, carbon deposits can be timely eliminated, which can well explain the reported experimental facts that CuNi bimetallic catalysts with Cu surface enrichment display excellent carbon-resistance ability in CH_4/CO_2 reforming.

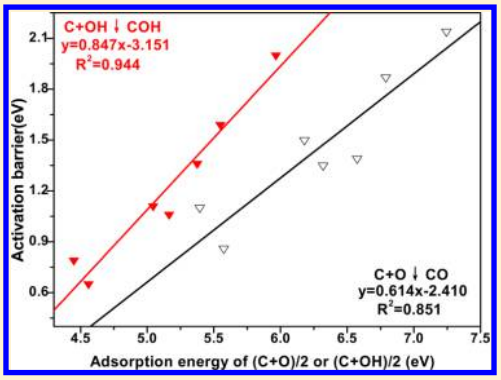

1. INTRODUCTION

Catalytic reforming of CH_4 with CO_2 provides potential incentives with great industrial and environmental attractiveness.[1−9] Nowadays, Ni-based catalyst has been considered to be of potential for industrial application due to high activity and wide availability. However, rapid coke accumulation on Ni-based catalyst and coke-induced deactivation are the main drawbacks to its industrialization.[10,11]

Coke accumulation on Ni-based catalyst is the result of carbon formation and carbon elimination.[12] Therefore, it is significantly necessary to investigate the underlying mechanism of carbon formation and elimination in CH_4/CO_2 reforming. For carbon formation, previous studies have shown that CH_4 complete dissociation is dominantly responsible for carbon formation in CH_4/CO_2 reforming,[13−16] thus, a large number of studies have focused on CH_4 dissociation to explore carbon formation on various Ni-based catalysts.[17−26] For carbon elimination, previous studies have suggested that the oxygenate intermediates, such as O and OH species (O from CO_2 dissociation, and OH from RWGS and H-assisted CO_2 dissociation, can act as surface cleaner to scavenge the deposited carbon.[27−29] Therefore, C + O and C + OH reactions are believed to be the key step to understand carbon elimination. However, to the best of our knowledge, few studies about carbon elimination on Ni-based catalyst have been reported.

Nowadays, many efforts have been devoted to improving the stability and carbon-resistance ability of Ni-based catalyst. An effective way to enhance resistance toward coke deposits is to introduce a second metal component to form bimetallic Ni-based catalyst.[30] It has been demonstrated that the presence of noble metals for the bimetallic Ni-based alloys can noticeably improve the stability of catalysts.[31,32] However, restricted availability and high cost limit their use in this process. Thus, many researchers have shifted their focuses to the combinations of non-noble metal (Cu, Fe, *etc.*) with Ni as inexpensive alternatives.[33] Wang et al.[34] reported that Fe incorporated into Ni-phase can stabilize the active nickel species, and make the

Received: February 12, 2015
Revised: June 1, 2015
Published: June 2, 2015

DOI: 10.1021/acs.jpcc.5b03868
J. Phys. Chem. C 2015, 119, 14135−14144

metal particle uniform distribution. Provendier and co-workers[35,36] proposed that FeNi alloy prevents carbon poisoning through a dilution effect on Ni particles. Wang et al.[37] predicted that Fe has cocatalytic function. Since Fe has high oxygen affinity than Ni,[38] the oxygen atoms on Fe species can be supplied to Ni species, which may promote the reaction between carbonaceous species and oxygen species, and suppresses carbon deposition.

Another important active phase promoter in CH_4/CO_2 reforming is Cu, the incorporation of Cu into Ni can interrupt the Ni−Ni network, and promote CH_4 cracking process, thus, the incorporation of Cu greatly reduces carbon deposition,[39−41] which is in agreement with the previous DFT calculations that of CuNi alloy can inhibit CH_4 dissociation to prevent carbon formation.[25,26] Tavares et al.[42] have pointed out that the stability of CuNi alloy cannot be fully explained by the ensemble effect of Cu on Ni metal that may inhibit the carbon formation rate on Ni catalyst. The same observation is reported by Chen et al.,[43] who showed that the incorporation of Cu into Ni affects the oxidation pathway of the deposited carbon, and this factor would be more important in the stability control of CuNi alloy.

Above results indicate that Cu and Fe promoters might block Ni sites that are necessary for activation of methane; However, Cu and Fe promoters can effectively prevent carbon poisoning through a dilution effect on Ni particles, meanwhile, the oxophililc nature of Fe and the effect of C oxidation pathway by Cu may be served as another important factor of their resistance to carbon deposition. Up to now, the roles of Cu and Fe promoters played in carbon elimination and the beneficial effects of bimetallic catalyst on carbon elimination have not been elucidated at the molecular level, which need to be clarified.

On the other hand, the arrangement of active component and the surface morphology of CuNi and FeNi alloys are obviously affected by the reacting atmosphere and temperature. Cu and Fe tend to form the homogeneous structures with Ni in CuNi and FeNi alloys.[40,44−47] However, under the certain condition, Cu or Fe is inclined to segregate on the surface of CuNi and FeNi alloys as a function of temperature and working circumstances.[37,48−51] Wang et al.[37] experimentally observed that Fe tends to enrich on the surface of FeNi alloy, and the segregated surface of FeNi(111) with Fe surface enrichment is mainly maintained during the reaction. The segregated surface of CuNi alloy with Cu surface enrichment is also evidenced by many researchers,[49−51] and the segregated CuNi surface structure displays better anticarbon deposit ability.[49−53] By hydrogen chemisorption and FTIR spectroscopy of CO adsorption, Kitla et al.[52] clearly demonstrated that the surface of CuNi bimetallic particles is strongly enriched by Cu, and Cu surface enrichment markedly reduces coking occurring preferentially on Ni-based catalyst, moreover, the ability of CH_4 activation is still maintained. Surface segregation of Cu in NiCu alloy also has been detected by Popova et al.,[53] who indicated that CuNi catalyst effectively resists the carbon deposition. These results show that the segregation of Cu and Fe modifies the surface morphology of Ni-based alloy, then, the modification of surface morphology will in turn have an effect on the adsorption properties of key intermediates, further on the reactivity of the deposited carbon with oxygen intermediates.[54,55] However, up to now, the underlying mechanisms about carbon elimination and the surface structure effects of CuNi(111) and FeNi(111) on carbon elimination remain unclear. As a result, a detailed mechanism investigation of C + O and C + OH reactions on different surface structures of CuNi(111) and FeNi(111) at the atomic scale will help us understand carbon elimination, as well as the effects of surface structure on carbon elimination, which is a necessary progress in the design of anticoking Ni-based catalyst.

In this study, we have systematically investigated the mechanism of C + O and C + OH reactions on the alloy CuNi(111) and FeNi(111) with the homogeneous and segregated surfaces, respectively; here, the results are obtained by using periodic density functional theory (DFT) method. The effects of Cu and Fe doping on the adsorption of key intermediates involved in carbon elimination have been examined, the most favorable pathway of C + O and C + OH reaction, as well as the effects of CuNi(111) and FeNi(111) surface structure and second metal composition on C + O and C + OH reactions have been identified. The results of this work are expected to provide a microcosmic insight into the roles of Cu and Fe doping, and clarify the effects of surface Fe and Cu segregation on carbon elimination.

2. COMPUTATIONAL DETAILS

2.1. Surface Models. Previous studies have suggested that the supported FeNi and CuNi bimetallic catalysts with an approximate ratio of Ni/M (M = Fe, Cu) to one have beneficial effects on increasing carbon deposition resistance, which can improve the catalytic performance in the reforming of CH_4 with CO_2.[52,56] Meanwhile, experimental and theoretical work demonstrated that FeNi alloy retains an FCC structure when Fe content is no more than 60%.[57,58] According to XRD characterization, the formation of chemically ordered FCC FeNi alloy has been observed.[45] On the other hand, Hua et al.[40] and Lee et al.[47] suggested that CuNi alloy is formed after H_2 reduction. Therefore, two bulk models with similar molar ratio (M:Ni = 1:1) are constructed by replacing two Ni atoms in the 4Ni atom conventional cell with two M (M = Ni, Fe) atoms. For FeNi alloy, a = 3.480 Å, $b = c$ = 3.604 Å; for CuNi alloy, a = 3.545 Å $b = c$ = 3.551 Å. The calculated lattice constants are consistent with the previous theoretical calculations.[59]

MNi(111) surface is obtained by cutting MNi alloy along the [111] direction. A rectangular $(2\sqrt{3} \times 2)$ supercell with four layer composed of eight metal atoms at each layer is utilized to represent the MNi(111) surface. Meanwhile, a 12 Å vacuum slab is inserted into the direction perpendicular to the surface in order to separate the neighboring repeated slabs. In all calculations, the upper two layers and the adsorbed species are allowed to relax, and the bottom two layers in the slab models are frozen.

Herein, we set up the homogeneous FeNi(111) and CuNi(111) surfaces, which are denoted as 1:1 Fe surface and 1:1 Cu surface, respectively, as shown in Figure 1. However, since the reacting atmosphere and temperature have obvious effect on the surface morphology of MNi alloy; under the certain conditions, Cu or Fe is inclined to segregate on the surface, namely, the surface is enriched with Cu or Fe atoms; meanwhile, the surface M segregation for MNi alloy have been detected by many experimental studies.[37,48−53,60−62] As a result, the segregated MNi(111) with the Cu or Fe enriched surface has been constructed. We have considered all possible replacement modes of the surface Ni atoms with Cu or Fe atoms of the subsurface layer for the segregated FeNi(111) and CuNi(111) surfaces (see part 1 in the Supporting Information). Our results show that when two interval Ni atoms of the

DOI: 10.1021/acs.jpcc.5b03868
J. Phys. Chem. C 2015, 119, 14135−14144

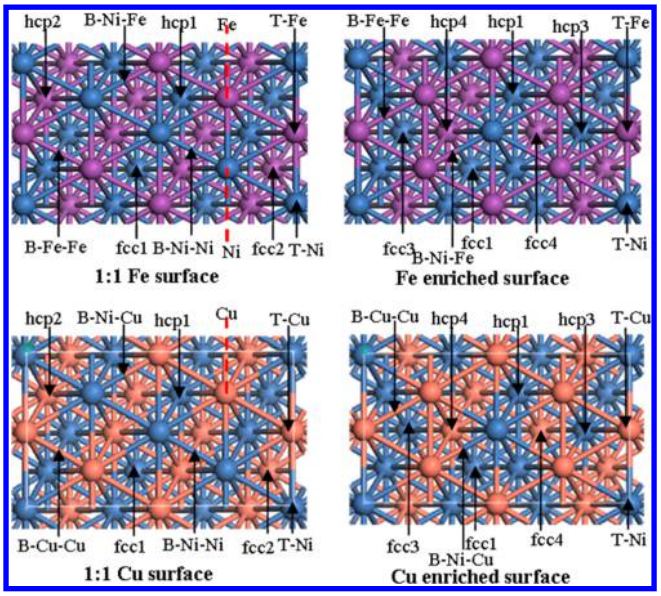

Figure 1. Surface morphology and the corresponding adsorption sites of the alloy NiCu(111) and NiFe(111) surfaces. Light sky blue, orange, and light purple balls stand for Ni, Cu, and Fe atoms, respectively.

surface layer are exchanged with two M atoms of the subsurface layer, the corresponding geometries of the segregated FeNi(111) and CuNi(111) surfaces is more stable than other geometries. Therefore, the segregated MNi(111) with the M-enriched surface are obtained by exchanging two interval Ni atoms of the surface layer with two M atoms of the subsurface layer, which are named as the Fe enriched surface and Cu enriched surface (see Figure 1), respectively. On the 1:1 M and the M-enriched surfaces, the numbers of M(Fe, Cu) atoms presented on the surface layer are 4 and 6, the corresponding surface coverage of M composition is equal to 1/2 and 3/4 ML, respectively, namely, the 1:1 M surface represent the homogeneous surface, and the M-enriched surfaces represent the segregated surface.

2.2. Computational Methods. All DFT calculations in this study have been carried out using the Vienna ab initio simulation package (VASP).[63,64] The projector augmented wave method (PAW)[65,66] is used to describe the ionic cores and their interaction with the valence electrons. The exchange-correlation energy is described by Perdew–Burke–Ernzerhof functional within the generalized gradient approximation (GGA-PBE).[67] A plane wave basis set with a kinetic energy cutoff of 400 eV is employed for the valence electrons. A Fermi smearing of 0.1 eV is utilized to determine electronic occupancies. Brillouin zone is sampled with a grid of 4 × 4 × 1 mesh points according to the Monkhorst–Pack procedure. Since two magnetic elements of Ni and Fe are involved in the system, the spin-polarized has been considered. Forces below 0.01 eV/Å are used as the criterion for the relaxation convergence. The relaxation of the electronic degrees of freedom is thought to be converged when the energy differences are less than 10^{-6} eV. The climbing-image nudged elastic band method (CI-NEB) has been employed to locate

Table 1. Adsorption Energies (eV) of the Species Involved in Carbon Elimination on the Pure Ni(111) and the Alloy FeNi(111) Surface[a]

		species				
surfaces	sites	C	O	OH	CO	COH
Ni(111)[73]	hcp	**−6.88**	−5.64	−3.35	**−1.89**	**−4.39**
	fcc	−6.83	**−5.76**	**−3.45**	−1.87	**−4.39**
	B	(hcp)[b]	(hcp)	(fcc)	−1.76	(fcc)
	T	(fcc)	(hcp)	(fcc)	−1.53	(hcp)
1:1 Fe surface	hcp1	−6.84	−6.20	**−3.90**	−1.67	−4.26
	hcp2	**−6.85**	−5.94	−3.57	−1.69	−4.27
	fcc1	**−6.85**	**−6.30**	**−3.90**	**−1.76**	−4.27
	fcc2	−6.81	−6.03	−3.64	−1.62	**−4.28**
	B–Ni–Ni	(hcp1)	(fcc2)	(fcc2)	(fcc1)	(hcp1)
	B–Ni–Fe	(hcp1)	(hcp2)	(hcp1)	(fcc1)	(fcc2)
	B–Fe–Fe	(hcp1)	(fcc1)	(fcc1)	T-Fe	(fcc2)
	T–Fe	(fcc1)	(fcc2)	(fcc2)	−1.63	(fcc2)
	T–Ni	(fcc2)	(fcc2)	(fcc1)	−1.53	(fcc2)
Fe-enriched surface	hcp1	−6.98	−6.18	−3.74	(B–Ni–Fe)	−4.36
	hcp3	**−7.07**	−6.45	−3.99	−1.68	**−4.38**
	hcp4	−7.00	−6.22	−3.74	(B–Ni–Fe)	−4.35
	fcc1	−6.93	−6.21	−3.75	(B–Ni–Fe)	−4.35
	fcc3	−7.00	**−6.51**	**−4.03**	(T–Fe)	−4.36
	fcc4	−6.96	−6.22	−3.76	(B–Ni–Fe)	−4.37
	B–Ni–Fe	(fcc4)	(fcc4)	(fcc4)	−1.71	(hcp1)
	B–Fe–Fe	(fcc3)	(hcp3)	(fcc4)	(T-Fe)	(fcc4)
	T–Fe	(hcp3)	(fcc3)	(hcp4)	**−1.72**	(hcp1)
	T–Ni	(fcc1)	(fcc4)	(fcc3)	(B–Ni–Fe)	(fcc4)

[a]The energies in bold are the adsorption energies at the most stable adsorption sites. [b]The adsorption sites presented in parentheses are the stable adsorption site of species, namely, the initial adsorption configurations of species putted initially at the corresponding sites are relaxed to the adsorption sites presented in parentheses after geometry optimization; for example, C initially adsorbed at the bridge site are converted that adsorbed at the hcp site after geometry optimization.

DOI: 10.1021/acs.jpcc.5b03868
J. Phys. Chem. C 2015, 119, 14135–14144

Table 2. Adsorption Energies (eV) of the Species Related to Carbon Elimination on the Alloy CuNi(111) Surface[a]

surfaces	site	species				
		C	O	OH	CO	COH
the 1:1 Cu surface	hcp1	(B−Ni−Ni)[b]	−5.00	−2.95	(T−Ni)	−4.27
	hcp2	(B−Ni−Ni)	−5.54	(B−Ni−Ni)	(B−Ni−Ni)	**-4.31**
	fcc1	(B−Ni−Ni)	−5.10	−3.13	(B−Ni−Ni)	−3.55
	fcc2	(B−Ni−Ni)	**-5.63**	(B−Ni−Ni)	(B−Ni−Ni)	−4.27
	B−Ni−Ni	**−6.73**	(fcc2)	**−3.36**	**−1.92**	(hcp2)
	B−Ni−Cu	(B−Ni−Ni)	(hcp2)	(fcc1)	(fcc1)	(hcp2)
	B−Cu−Cu	(B−Ni−Ni)	(fcc1)	(fcc1)	(T-Ni)	(hcp2)
	T−Cu	(B−Ni−Ni)	(fcc2)	(fcc1)	(B−Ni−Ni)	(hcp2)
	T−Ni	(B−Ni−Ni)	(fcc2)	(B−Ni−Ni)	−1.62	(fcc1)
the Cu enriched surface	hcp1	−5.76	−5.11	−3.12	(T−Ni)	−3.55
	hcp3	−4.81	−4.61	−2.86	−0.75	−2.74
	hcp4	**−5.88**	−5.14	−3.19	(T−Ni)	**−3.67**
	fcc1	−5.78	−5.21	−3.20	(T−Ni)	−3.59
	fcc3	−4.84	−4.75	−3.04	−0.89	−2.85
	fcc4	(B−Ni−Cu)	**−5.27**	**−3.24**	(T−Ni)	−3.53
	B−Ni−Cu	−5.86	(hcp4)	(hcp4)	(T−Ni)	(fcc1)
	B−Cu−Cu	(B−Ni−Cu)	(hcp4)	(hcp4)	(T−Ni)	(hcp4)
	T−Cu	(B−Ni−Cu)	(fcc3)	(fcc4)	(T−Ni)	(hcp1)
	T−Ni	(B−Ni−Cu)	(hcp4)	(hcp1)	**−1.68**	(fcc1)

[a]The energies in bold are the corresponding adsorption energies at the most stable adsorption sites. [b]The adsorption sites presented in parentheses are the stable adsorption site of species; namely, the initial adsorption configurations of species putted initially at the corresponding sites are relaxed to the adsorption sites presented in parentheses after geometry optimization.

the saddle points.[68] Transition states have been optimized using the dimer method.[69,70] The transition state structures are assumed to be converged if the forces acting on the atoms are all less than 0.05 eV/Å for the various degrees of freedom set in the calculation.

The adsorption energy, E_{ads}, is calculated by

$$E_{ads} = E_{(adsorbate/slab)} - E_{slab} - E_{adorbate}$$

where $E_{adsorbate/slab}$ is the total energy of the slab model with adsorbate; E_{slab} is the total energy of the bare slab model; $E_{adsorbate}$ is the total energy of the isolated adsorbate obtained in a 10 × 10 × 10 Å cubic box.

3. RESULTS AND DISCUSSION

3.1. Adsorption of Reaction Species. For Ni(111) surface,[71,72] four different adsorption sites exist: hexagonal-close-packed (hcp), face-centered-cubic (fcc), top (T), and bridge (B). On MNi(111) surface, several additional sites are formed due to the existence of two compositions in the lattice, as displayed in Figure 1. All possible adsorption sites on MNi(111) surface have been considered in this study, the adsorption energies for each species at their stable adsorption sites on FeNi(111) and CuNi(111) surfaces are summarized in Tables 1 and 2, and the corresponding adsorption configurations are displayed in part 2 of Supporting Information. In addition, our previous studies have investigated the possible adsorption sites of related species involved in carbon elimination on Ni(111) surface,[73] which is also listed in Table 1.

3.1.1. C Adsorption. On Ni(111), the most stable site of C atom is hcp site with an adsorption energy of −6.88 eV, which agrees with the values obtained by Fan et al.[74] On FeNi(111), the Fe segregation for the Fe enriched surface increases the adsorption ability of C atom. On CuNi(111), for the 1:1 Cu surface, the most stable adsorption site of C atom is bridge site composed of two Ni atoms, which is consistent with the previous studies;[75] the introduction of Cu into Ni weakens the adsorption stability of C, which may increase the diffusion ability of C species to interact with O and OH species, further promotes carbon elimination.

3.1.2. O and OH Adsorption. On FeNi(111), compared to Ni(111), the introduction of Fe into Ni enhances the adsorption ability of O and OH species. Meanwhile, the increased degree of O adsorption energy far outstrips C adsorption on FeNi(111), indicating that Fe has stronger affinity for oxygen species than carbon species, which agrees with the previous experimental predictions.[37,38]

On CuNi(111), the introduction of Cu into Ni decreases the adsorption ability of O and OH species, which may increase the diffusion ability of O and OH species to interact with C species, further improve the ability of carbon elimination. In addition, compared to Ni(111), the diffusion of single O or OH species from the their most stable adsorption site to the adjacent stable site has indicated that the diffusion of single O or OH species is obviously promoted on the Cu enriched surface, which may be in favor of carbon elimination (see part 3 in the Supporting Information).

3.1.3. COH and CO Adsorption. For COH adsorption, COH species adsorbed on the alloy FeNi(111) and CuNi(111) is energetically unfavorable than that on Ni(111). Thus, the introduction of Fe or Cu into Ni reduces the adsorption stability of COH species.

For CO adsorption, on Ni(111), CO prefers to adsorb at the hcp site with an adsorption energy of −1.89 eV, which agrees with the previous DFT studies.[71,76] On FeNi(111) surface, the adsorption energy of CO is larger than that on Ni(111), indicating that the introduction of Fe into Ni weakens the adsorption ability of CO. On CuNi(111) surface, the 1:1 Cu surface slightly increase the adsorption ability of CO, whereas the Cu enriched surface reduces the adsorption stability of CO, which agrees with the previous experimental observation.[52]

DOI: 10.1021/acs.jpcc.5b03868
J. Phys. Chem. C 2015, 119, 14135−14144

In addition, the adsorption of related species on the pure Cu(111) and Fe(110) have been considered (see Part 4 in the Supporting Information). Our results indicate that compared to Ni(111), C, O, OH, CO and COH species adsorbed on Cu(111) is energetically unfavorable; on Fe(110), the adsorption energy of C, O and OH species is significantly increased, the adsorption energy of CO is decreased, and COH adsorbed on Fe(110) is slightly favorable compared to Ni(111). These results are in good agreement with those obtained on the alloy MNi (M = Fe, Cu) surfaces.

3.2. C + O and C + OH Reactions for Carbon Elimination. In order to illuminate the mechanism of carbon elimination in detail, various possible paths of C + O(OH) reaction have been considered. For the coadsorption configurations of C + O(OH), we not only consider the coadsorption configurations binding at their most favorable site, but also examine other possible coadsorption configurations adsorbed at their metastable sites due to the small difference of adsorption energy for C, O and OH species, as shown in Figure 2.

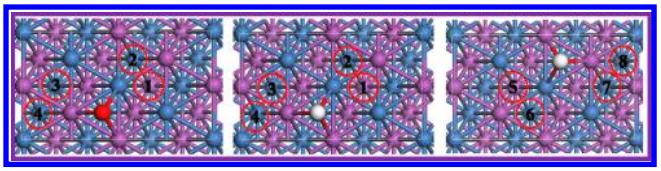

Figure 2. Possible coadsorption configurations of C + O or C + OH on the 1:1 Fe surface of FeNi(111).

The configurations of initial states (ISs), transition states (TSs), and final states (FSs) for carbon elimination reactions involving in all possible pathways on the alloy MNi surfaces are displayed in the Part 5 of Supporting Information. The activation barriers and reaction energies of C + O and C + OH reactions with different pathways are listed in Table 3. The potential energy profile for the most favorable pathway of C + O and C + OH reactions on the pure Ni(111) and the alloy MNi(111) (M = Fe, Cu) surfaces has been presented in Figure 3.

On FeNi(111), the most favorable path of C + O reaction needs to overcome the activation barriers of 1.39 and 1.87 eV

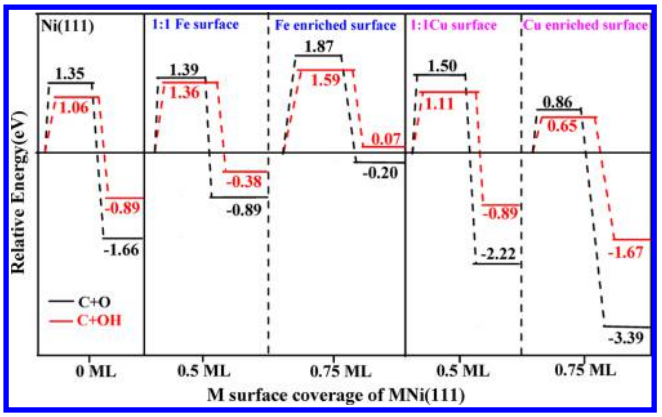

Figure 3. Potential energy profile for the most favorable pathway of C + O and C + OH reactions on the pure Ni(111) and the alloy MNi(111) (M = Fe, Cu) surfaces.

on the 1:1 Fe and the Fe enriched surfaces, respectively, which are higher by 0.04 and 0.52 eV than that on Ni(111), indicating that the introduction of Fe into Ni goes against C + O reaction; for C + OH → COH reaction, the activation barrier (1.36 and 1.59 eV) of the most favorable path on the 1:1 Fe and the Fe enriched surfaces are still higher than (1.06 eV) on Ni(111), suggesting that the introduction of Fe into Ni also restrains the C + OH reaction. Meanwhile, it is noted that the activation barrier of C + O(OH) reaction on the Fe enriched surface is much higher than that on the 1:1 Fe surface, namely, the surface Fe segregation of FeNi(111) inhibits carbon elimination.

On CuNi(111), the activation barriers of the most favorable path for C + O and C + OH reactions on the 1:1 Cu surface (1.50 and 1.11 eV) are higher than those (1.35 and 1.06 eV) on Ni(111), namely, compared to Ni(111), the 1:1 Cu surface restrains C + O and C + OH reactions. However, the activation barrier of the most favorable path for C + O reaction on the Cu enriched surface is 0.86 eV, which is lower by 0.49 eV than that on Ni(111); for C + OH reaction, the activation barrier (0.65 eV) of the most favorable path is still lower by 0.41 eV than that on Ni(111), indicating that C + O and C + OH reaction are accelerated on the Cu enriched surface, namely, CuNi(111) with the segregated Cu surface is beneficial for carbon

Table 3. Activation Energies (E_a/eV) and Reaction Energies (ΔH/eV) of C + O and C + OH Reactions on the Pure Ni(111) and the Alloy NiM (M = Fe, Cu) Surfaces

		Ni(111)[70]		FeNi(111)				CuNi(111)			
				1:1 Fe surface		Fe-enriched surface		1:1 Cu surface		Cu-enriched surface	
reactions	paths	E_a	ΔH	E_a	ΔH	E_a	ΔH	E_a	ΔH	E_a	ΔH
C + O → CO	path 1	2.29	−1.50	**1.39 (1.37)**	**-0.89**	**1.87 (1.83)**	**−0.20**	**1.50 (1.47)**	**−2.22**	1.19	−3.16
	path 2	**1.35 (1.33)**	**−1.66**	1.80	−0.83	4.84	−0.25			0.92	−3.37
	path 3			1.42	−0.96					**0.86 (0.84)**	**−3.39**
	path 4			1.69	−0.65						
C + OH → COH	path 1	1.26	−0.74	1.37	−0.38	1.67	0.18	**1.11 (1.08)**	**-1.04**	0.70	−1.56
	path 2	**1.06(1.04)**[a]	**-0.89**	1.48	−0.30	**1.59 (1.58)**	**0.07**			**0.65 (0.63)**	**−1.67**
	path 3			1.51	−0.25					0.83	−1.31
	path 4			1.61	−0.11					0.72	−1.56
	path 5			1.56	−0.30						
	path 6			**1.36 (1.36)**	**−0.38**						
	path 7			1.41	−0.25						
	path 8			1.49	−0.16						

[a]The values presented in parentheses are the activation energies with ZPE correction.

DOI: 10.1021/acs.jpcc.5b03868
J. Phys. Chem. C 2015, 119, 14135−14144

elimination, which is in agreement with the experimental results that the introduction of Cu into Ni may facilitate C oxidation.[43]

In general, as shown in Figure 3, on Ni(111), FeNi(111), and CuNi(111) surfaces, the introduction of Fe into Ni goes against carbon elimination; the introduction of Cu into Ni to form the 1:1 Cu surface restrains carbon elimination, however, the Cu enriched surface can accelerate carbon elimination, in which the activation barriers of C + O and C + OH reactions on the Cu enriched surface are the lowest among all considered surfaces, indicating that carbon deposits can be easily eliminated by O and OH species on CuNi(111) with the segregated Cu surface. Moreover, the activation barriers of C + OH reaction are lower than those of C + O reaction, which means that OH species is more effective for carbon elimination than O species.

Segregation is a common process that occurs in many multicomponent catalysts such as NiCu alloy. Cu segregation in NiCu bimetallic catalysts have been confirmed by many experimental studies, and the CuNi catalyst with the segregated Cu surface displays better anticarbon deposit ability; for example, Naghash and his co-workers[62] have indicated that Cu has a tendency to segregate in order to reduce the interfacial surface energies based on the analysis of XRD, XPS, BE, and Auger measurements. By means of XRD, XPS, EXAFS, and FMR, Wang et al.[61] found that the surface concentration of Cu is higher than the concentration of Ni by a factor of 2−3 in CuNi bimetallic catalysts. Tavares et al.[50] have observed that Cu tends to enrich on the surface of CuNi alloy particles, and the incorporation of Cu into Ni can decrease the carbon formation. The CuNi alloy with surface Cu enrichment is also evidenced by La Rosa et al.,[51] which showed that no significant carbon deposition has been observed after operation for 2000 h. By hydrogen chemisorption and FTIR spectroscopy of CO adsorption, Kitla et al.[52] clearly demonstrated that the surface of CuNi bimetallic particles is strongly enriched by Cu, and surface Cu enrichment markedly reduces coking occurring preferentially on Ni-based catalyst, while maintaining methane activation. Surface segregation of Cu in NiCu alloy has also been detected by Popova et al.,[53] who indicated that the CuNi catalyst effectively resists the carbon deposition. Therefore, on the basis of above experimental studies, we can believe that CuNi alloy with surface Cu enrichment, namely, CuNi alloy with the segregated Cu surface, can exist in the real catalytic system.

In addition, C + O and C + OH reactions on the pure Cu(111) and Fe(110) surfaces have been calculated (see part 6 in the Supporting Information), the results show that compared to Ni(111), C + O and C + OH reactions are accelerated on Cu(111), while both are obviously restrained on Fe(110); these results are consistent with those obtained on the alloy MNi (M = Fe, Cu) surfaces.

3.3. Relationship between the Adsorption Energy of C + O(OH) and Carbon Elimination Reaction. In order to provide further insight into the controlling factors in carbon elimination, the adsorption property of surface species (e.g., the adsorption energy of C, O, and OH species on the metal surface) has been considered to correlate with the activation barrier of carbon elimination on the pure Ni(111), Cu(111), and Fe(110), as well as four types of the alloy MNi (M = Fe, Cu) surfaces. Figure 4 presents the relationship between the activation barrier change of carbon elimination reaction on different metal surfaces and the average adsorption energy of C and O(OH) species on the corresponding metal surface.

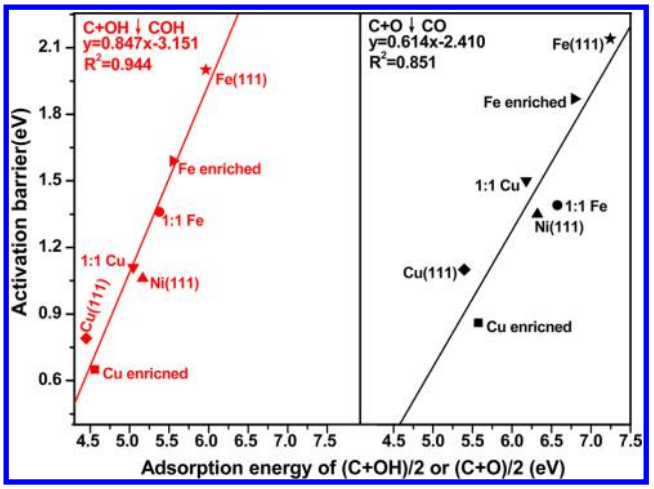

Figure 4. Relationship between activation barrier change of carbon elimination reaction at different metal surfaces and the average adsorption energy of C and O(OH) species on the metal surface.

From our calculated results, we can obtain a general rule: the larger the average adsorption energy of C + O or C + OH species on the metal surface is, the larger the activation barrier of C + O or C + OH reactions on the metal surface is namely, the more strongly bound the C + O or C + OH species on the metal surface is, the less the promoting effect or the stronger the inhibiting effect for carbon elimination. Moreover, a good linear relationship between the average adsorption energy of C + O or C + OH species and the activation barrier of C + O or C + OH reactions for carbon reaction is found (Figure 4). Especially, a very good linear relationship exists between the average adsorption energy of C + OH species ($E_{ads(C+OH)/2}$) and the activation energy of C + OH reaction due to the high R^2 value (0.944). In general, the ability of carbon elimination on the metal surface increases with the decreasing of adsorption ability for C + O and C + OH species on the corresponding metal surface.

In addition, for the C deposition, previous studies have shown that CH_4 complete dissociation is responsible for carbon formation in CH_4/CO_2 reforming. Therefore, a large number of studies have focused on CH_4 dissociation to explore carbon formation on various Ni-based catalysts, which presents the C deposition trends. For example, Liu et al.[59] have found the linear relationship between the activation energy of CH_4 dissociation and the adsorption energy of C atom, suggesting that the activation energy of CH_4 dissociation decreases with the increase of the adsorption energy of C atom. The same observation is confirmed by Fan et al.,[21] indicating that the larger the adsorption energy of C atom is, the easier CH_4 first dissociation step (the rate-determining step) is. Therefore, the decrease of C adsorption energy may restrain CH_4 dissociation and decrease the C formation by CH_4 dissociation.

On the basis of the above analysis, the trends of C elimination and C deposition are linked closely with the adsorption energy of C. For example, when C adsorption energy increases, the average adsorption energy of C + O and C + OH increases, and carbon elimination is inhibited; meanwhile, carbon formation by CH_4 dissociation is promoted due to the decreased activation energy of CH_4 dissociation; as a result, C deposition is likely to occur on the catalyst surface and to reduce the stability of the catalyst. Therefore, the adsorption energy of C on the catalyst surface could be a good descriptor

DOI: 10.1021/acs.jpcc.5b03868
J. Phys. Chem. C 2015, 119, 14135−14144

Table 4. Rate Constant k (s^{-1}) of C + O(OH) Reaction at Different Temperature on the Pure Ni(111) and the Alloy MNi(111) (M = Fe, Cu) Surfaces

surfaces	reactions	rate constant k (s^{-1}) 800 K	850 K	900 K	950 K	1000 K
Ni(111) surface	C + O → CO	9.38×10^4	3.15×10^5	9.28×10^5	2.45×10^6	5.87×10^6
	C + OH → COH	6.59×10^6	1.72×10^7	4.06×10^7	8.77×10^7	1.76×10^8
1:1 Fe surface	C + O → CO	1.09×10^5	3.77×10^5	1.14×10^6	3.1×10^6	7.61×10^6
	C + OH → COH	4.1×10^4	1.39×10^5	4.1×10^5	1.09×10^6	2.62×10^6
Fe-enriched surface	C + O → CO	3.02×10^2	1.57×10^3	6.82×10^3	2.54×10^4	8.34×10^4
	C + OH → COH	6.24×10^3	2.57×10^4	9.05×10^4	2.80×10^5	7.77×10^5
1:1 Cu surface	C + O → CO	1.91×10^4	7.23×10^4	2.37×10^5	6.89×10^5	1.80×10^6
	C + OH → COH	6.88×10^6	1.87×10^7	4.58×10^7	1.02×10^8	2.11×10^8
Cu-enriched surface	C + O → CO	8.69×10^8	1.91×10^9	3.88×10^9	7.32×10^9	1.30×10^{10}
	C + OH → COH	3.41×10^9	6.26×10^9	1.08×10^{10}	1.76×10^{10}	2.74×10^{10}

for evaluating the catalyst stability, and an effective strategy to improve the coke resistance of Ni catalyst is to weaken the C adsorption strength on the catalyst.

3.4. Effect of Temperature on C + O and C + OH Reactions on the Alloy MNi Surface. Under the realistic conditions, the reforming of CH_4 with CO_2 is a highly endothermic reaction, which requires the operating temperatures of 800−1000 K to obtain the high equilibrium conversion of CH_4 and CO_2 and to prevent carbon deposition.[77] Therefore, to further understand the effect of temperature on C + O(OH) reaction over Ni(111) and the alloy MNi(111) (M = Fe, Cu) surfaces, we have calculated the rate constants for the most favorable path of C + O(OH) reaction at the temperatures of 800, 850, 900, 950, and 1000 K, respectively, the corresponding results are listed in Table 4. The detailed descriptions of rate constant calculation has presented in the Part 7 of Supporting Information.

We can see that the rate constant k of C + O(OH) reaction increases with the increasing of temperature on Ni(111) and the alloy MNi surfaces, respectively. At the same temperature, on Ni(111), CuNi(111) surface and FeNi(111) with the Fe enriched surface, the rate constants of C + OH reaction are larger than the corresponding values of C + O reaction, suggesting that OH species is more effective for carbon elimination than O species. However, on FeNi(111) with the 1:1 Fe surface, O species is more favorable than OH species for carbon elimination.

On FeNi(111), at the same temperature, for C + O reaction, the rate constant is in the order of the 1:1 Fe surface > Ni(111) > the Fe enriched surface, namely, C + O reaction is accelerated on the 1:1 Fe surface, while it is obviously restrained on the Fe enriched surface; for C + OH reaction, the rate constant is in the order of Ni(111) > the 1:1 Fe surface > the Fe enriched surface, indicating that FeNi(111) surface inhibits the C + OH reaction. More interestingly, the rate constants of C + OH reaction on Ni(111) is much larger than that of C + O reaction on the 1:1 Fe surface. Therefore, compared to Ni(111), FeNi(111) surface goes against carbon elimination, namely, carbon deposits cannot be effectively improved on the alloy FeNi(111) surface.

On CuNi(111), at the same temperature, for C + O reaction, the rate constant is in the order of the Cu enriched surface > Ni(111) > the 1:1 Cu surface, namely, the C + O reaction is restrained on the 1:1 Cu surface, while it is accelerated on the Cu enriched surface; for C + OH reaction, the rate constant is in the order of the Cu enriched surface > the 1:1 Cu surface > Ni(111), suggesting that C + OH reaction is promoted on CuNi(111) surface. Moreover, the rate constants of C + O(OH) reaction on the Cu enriched surface are much larger than those on the 1:1 Cu surface and Ni(111), which means that CuNi(111) with the segregated Cu surface is obviously beneficial for carbon elimination. As a result, carbon deposits can be easily eliminated by O and OH species on the segregated CuNi(111) with Cu enriched surface.

3.5. Effect of Fe and Cu on the Entire Catalytic Cycle in CH_4/CO_2 Reforming. Up to now, many theoretical and experimental studies have been carried out to understand carbon formation by probing into CH_4 dissociation on Ni-based bimetallic catalysts.[15−28,44,59,75] Fan and his co-workers[44] have shown that C concentration on the alloy FeNi surface is predicted to increase with the increasing of Fe content, which agrees with our results that alloy FeNi(111) surface is not in favor of carbon elimination, thus, carbon deposition is likely to occur on FeNi alloy. On the other hand, the studies by Liu et al.[59,75] have shown that compared to Ni(111), carbon formation by CH_4 dissociation is promoted on FeNi(111) and the homogeneous CuNi(111) surface, while it is suppressed on the segregated CuNi(111) surface. Our results show that on CuNi alloy, carbon elimination is favorable, among the different CuNi alloy surfaces, on the homogeneous CuNi(111) surface, the extent of carbon deposition depends on the relative rate of carbon formation and carbon elimination, however, on the segregated CuNi(111) surface, carbon formation by CH_4 dissociation is inhibited, and carbon elimination is accelerated. Therefore, once carbon deposition occurs on the segregated CuNi(111) with the Cu enriched surface, carbon deposition can be timely eliminated. An efficient periodic cycle of carbon formation and elimination on the segregated CuNi alloy with the Cu enriched surface may be one of the contributions leading to the stable catalytic performance. These calculated results well explain the experimental facts that the segregated CuNi bimetallic catalysts with the Cu enriched surface have excellent catalytic performance and carbon-resistance ability in CH_4/CO_2 reforming.[49−53]

4. CONCLUSIONS

In this work, using density functional theory calculations, we have systematically investigated the adsorption of C, O, CO, OH and COH species as well as the mechanism of C + O(OH) involved in carbon elimination on FeNi(111) and CuNi(111) surfaces. For FeNi(111) and CuNi(111) surfaces, the homogeneous and segregated surfaces have been considered. Our results show that OH species has a stronger ability of carbon eliminating than O species on Ni(111), CuNi(111)

DOI: 10.1021/acs.jpcc.5b03868
J. Phys. Chem. C 2015, 119, 14135−14144

surface and FeNi(111) with the segregated surface; however, on FeNi(111) with the homogeneous surface, O species is more preferred. The surface structures of CuNi(111) and FeNi(111) have obvious effect on C + O(OH) reaction of carbon elimination. Compared to Ni(111) surface, FeNi(111) surface restrains carbon elimination, while CuNi(111) surface promotes carbon elimination, especially for the segregated CuNi(111) with Cu surface enrichment, carbon formation is inhibited, and carbon elimination is accelerated; as a result, an efficient periodic cycle of carbon formation and elimination on the segregated CuNi alloy with Cu surface enrichment may be responsible for the stability of CuNi bimetallic catalysts. Moreover, a good linear relationship exists between the average adsorption energy of C + O or C + OH species and the activation barrier of C + O or C + OH reactions for carbon reaction is found, namely, the ability of carbon elimination on the metal surface increases with the decreasing of adsorption ability for C + O and C + OH species on the corresponding metal surface.

■ ASSOCIATED CONTENT

Supporting Information

Descriptions about model construction of the segregated MNi(111) (M = Cu, Fe) with the M-enriched surface, the stable configurations of reaction species and the C + O and C + OH reactions on MNi(111), O and OH diffusion on Ni(111) and CuNi(111) surface, the stable configurations of reaction species and the C + O and C + OH reactions on Cu(111) and Fe(110), and rate constant calculations have been presented in detail. The Supporting Information is available free of charge on the ACS Publications website at DOI: 10.1021/acs.jpcc.5b03868.

■ AUTHOR INFORMATION

Corresponding Author

*(B.J. Wang) Present Address: No. 79 Yingze West Street, Taiyuan 030024, China. Telephone: +86 351 6018239. Fax: +86 351 6041237. E-mail: quantumtyut@126.com; wangbaojun@tyut.edu.cn.

Notes

The authors declare no competing financial interest.

■ ACKNOWLEDGMENTS

This work is financially supported by the National Natural Science Foundation of China (Nos. 21276171, 21276003, and 21476155), the Natural Science Foundation of Shanxi Province (No. 2014011012-2), the Program for the Top Young Academic Leaders of Higher Learning Institutions of Shanxi, and the Top Young Innovative Talents of Shanxi Province. The authors especially thank two anonymous reviewers for their helpful suggestions on the quality improvement of our present paper.

■ REFERENCES

(1) Fan, M. S.; Abdullah, A. Z.; Bhatia, S. Catalytic Technology for Carbon Dioxide Reforming of Methane to Synthesis Gas. *ChemCatChem.* **2009**, *1*, 192−208.

(2) Bradford, M. C. J.; Vannice, M. A. CO_2 Reforming of CH_4. *Catal. Rev.* **1999**, *41*, 1−42.

(3) Ginsburg, J. M.; Piña, J.; Solhet, T.; El Lasa, H. I. Coke Formation over a Nickel Catalyst under Methane Dry Reforming Conditions: Thermodynamic and Kinetic Models. *Ind. Eng. Chem. Res.* **2005**, *44*, 4846−4854.

(4) Tomishige, K.; Chen, Y. G.; Yokoyama, K.; Fujimoto, K. Catalytic Performance and Catalyst Structure of Nickel−Magnesia Catalysts for CO_2 Reforming of Methane. *J. Catal.* **1999**, *184*, 479−490.

(5) Tang, S.; Ji, L.; Lin, J.; Zeng, H. C.; Tan, K. L.; Li, K. CO_2 Reforming of Methane to Synthesis Gas over Sol−Gel-made Ni/γ-Al_2O_3 Catalysts from Organometallic Precursors. *J. Catal.* **2000**, *194*, 424−430.

(6) Muradov, N.; Smith, F.; T-Raissi, A. Hydrogen Production by Catalytic Processing of Renewable Methane-rich Gases. *Int. J. Hydrogen Energy* **2008**, *33*, 2023−2035.

(7) Benito, M.; García, S.; Ferreira-Aparicio, P.; García Serrano, L.; Daza, L. Development of Biogas Reforming Ni−La−Al Catalysts for Fuel Cells. *J. Power Sources* **2007**, *169*, 177−183.

(8) Xu, L.; Song, H.; Chou, L. Carbon Dioxide Reforming of Methane over Ordered Mesoporous NiO−MgO−Al_2O_3 Composite Oxides. *Appl. Catal. B. Environ.* **2011**, *108*, 177−190.

(9) Kumar, P.; Sun, Y.; Idem, R. O. Comparative Study of Ni-based Mixed Oxide Catalyst for Carbon Dioxide Reforming of Methane. *Energy Fuel* **2008**, *22*, 3575−3582.

(10) Zhang, J.; Wang, H.; Dalai, A. K. Effects of Metal Content on Activity and Stability of Ni-Co Bimetallic Catalysts for CO_2 Reforming of CH_4. *Appl. Catal. A: Gen.* **2008**, *339*, 121−129.

(11) Vasileiadis, S.; Ziaka-Vasileiadou, Z. Biomass Reforming Process for Integrated Solid Oxide-Fuel Cell Power Generation. *Chem. Eng. Sci.* **2004**, *59*, 4853−4859.

(12) Trimm, D. L. Coke Formation and Minimisation during Steam Reforming Reactions. *Catal. Today* **1997**, *37*, 233−238.

(13) Tsang, S. C.; Claridge, J. B.; Green, M. L. H. Recent Advances in the Conversion of Methane to Synthesis Gas. *Catal. Today* **1995**, *23*, 3−15.

(14) Chen, D.; Lødeng, R.; Anundskås, A.; Olsvik, O.; Holmen, A. Deactivation during Carbon Dioxide Reforming of Methane over Ni Catalyst: Microkinetic Analysis. *Chem. Eng. Sci.* **2001**, *56*, 1371−1379.

(15) Djinović, P.; Črnivec, I. G. O.; Batista, J.; Pintar, A. Catalytic Syngas Production from Greenhouse Gasses: Performance Comparison of Ru-Al_2O_3 and Rh-CeO_2 Catalysts. *Chem. Eng. Process.* **2011**, *50*, 1054−1062.

(16) Črnivec, I. G. O.; Djinović, P.; Erjavec, B.; Pintar, A. Effect of Synthesis Parameters on Morphology and Activity of Bimetallic Catalysts in CO_2-CH_4 reforming. *Chem. Eng. J.* **2012**, *207*, 299−307.

(17) Zhang, J.; Wang, H.; Dalai, A. K. Effects of Metal Content on Activity and Stability of Ni-Co Bimetallic Catalysts for CO_2 Reforming of CH_4. *Appl. Catal. A: Gen.* **2008**, *339*, 121−129.

(18) Menegazzo, F.; Signoretto, M.; Pinna, F.; Pernicone, N. Optimization of Bimetallic Dry Reforming Catalysts by Temperature Programmed Reaction. *Appl. Catal. A: Gen.* **2012**, *439*, 80−87.

(19) Liu, H.; Zhang, R.; Yan, R.; Wang, B.; Xie, K. CH_4 Dissociation on NiCo(111) surface: A first-principles Study. *Appl. Surf. Sci.* **2011**, *257*, 8955−8964.

(20) Li, K.; Zhou, Z.; Wang, Y.; Wu, Z. A Theoretical Study of CH_4 Dissociation on NiPd(111) Surface. *Surf. Sci.* **2013**, *612*, 63−68.

(21) Fan, C.; Zhu, Y. A.; Xu, Y.; Zhou, Y.; Zhou, X. G.; Chen, D. Origin of Synergistic Effect over Ni-based Bimetallic Surfaces: A Density Functional Theory Study. *J. Chem. Phys.* **2012**, *137*, 014703−1−014703−10.

(22) Xu, Y.; Fan, C.; Zhu, Y. A.; Li, P.; Zhou, X. G.; Chen, D.; Yuan, W. K. Effect of Ag on the Control of Ni-catalyzed Carbon Formation: A Density Functional Theory Study. *Catal. Today.* **2012**, *186*, 54−62.

(23) Huang, Y.; Du, J.; Ling, C.; Zhou, T.; Wang, S. Methane Dehydrogenation on Au/Ni Surface Alloys−A First-principles Study. *Catal. Sci. Technol.* **2013**, *3*, 1343−1354.1.36.

(24) Nikolla, E.; Holewinski, A.; Schwank, J.; Linic, S. Controlling Carbon Surface Chemistry by Alloying: Carbon Tolerant Reforming Catalyst. *J. Am. Chem. Soc.* **2006**, *128*, 11354−11355.

(25) Wang, M.; Fu, Z.; Yang, Z. The Carbon-tolerance Mechanism of Ni-based Alloy with Coinage Metals. *Phys. Lett. A* **2013**, *377*, 2189−2194.

DOI: 10.1021/acs.jpcc.5b03868
J. Phys. Chem. C 2015, 119, 14135−14144

(26) An, W.; Zeng, X. C.; Turner, C. H. First-principles Study of Methane Dehydrogenation on A Bimetallic Cu/Ni(111) Surface. *J. Chem. Phys.* **2009**, *131*, 174702−1−174702−11.
(27) Solymosi, F.; Tolmacsov, P.; Zaka, T. S. Dry Reforming of Propane over Supported Re Catalyst. *J. Catal.* **2005**, *233*, 51−59.
(28) Siahvashi, A.; Adesina, A. A. Kinetic Study of Propane CO_2 Reforming over Bimetallic Mo−Ni/Al_2O_3 Catalyst. *Ind. Eng. Chem. Res.* **2013**, *52*, 15377−15386.
(29) Sutton, D.; Moisan, J. F.; Ross, J. R. H. Kinetic Study of CO_2 Reforming of Propane over Ru/Al_2O_3. *Catal. Lett.* **2001**, *75*, 175−181.
(30) Takanabe, K.; Nagaoka, K.; Nariai, K. Improved Resistance Against Coke Deposition of Titania Supported Cobalt and Nickel Bimetallic Catalysts for Carbon Dioxide Reforming of Methane. *Catal. Lett.* **2005**, *102*, 153−157.
(31) Hou, Z.; Yashima, T. Small Amounts of Rh-Promoted Ni Catalysts for Methane Reforming with CO_2. *Catal. Lett.* **2003**, *89*, 193−197.
(32) Meshkani, F.; Rezaei, M. Nanocrystalline MgO Supported Nickel-based Bimetallic Catalysts for Carbon Dioxide Reforming of Methane. *Int. J. Hydrogen Energy* **2010**, *35*, 10295−10301.
(33) Hu, Y. H. Advances in Catalysts for CO_2 Reforming of Methane. In Advances in CO_2 Conversion and Utilization. In *ACS Symposium Series*; American Chemical Society: Washington, DC; 2010.
(34) Wang, J.; Liu, C.; Zhang, Y.; Yu, K.; Zhu, X.; He, F. Partial Oxidation of Methane to Syngas over Glow Discharge Plasma Treated Ni−Fe/Al_2O_3 Catalyst. *Catal. Today* **2004**, *89*, 183−191.
(35) Provendier, H.; Petit, C.; Estournes, C.; Kiennemann, A. Stabilisation of Active Nickel Catalysts in Partial Oxidation of Methane to Synthesis Gas by Iron Addition. *Appl. Catal. A: Gen.* **1999**, *180*, 163−173.
(36) Provendier, H.; Petit, C.; Kiennemann, A. Steam Reforming of Methane on $LaNi_xFe_{1-x}O_3$ ($0 \leq x \leq 1$) Perovskites. Reactivity and Characterization after Test. *Surf. Chem. Catal.* **2001**, *4*, 57−66.
(37) Wang, L.; Li, D.; Koike, M.; Koso, S.; Nakagawa, Y.; Xu, Y. Catalytic Performance and Characterization of Ni-Fe Catalysts for the Steam Reforming of Tar from Biomass Pyrolysis to Synthesis Gas. *Appl. Catal. A: Gen.* **2011**, *392*, 248−255.
(38) Reed, T. B. *Free Energy Formation of Binary Compounds*; MIT Press: Cambridge, MA, 1971; pp 66−70.
(39) Faro, M. L.; Frontera, P.; Antonucci, P. L.; Aricò, A. S. Ni-Cu Based Catalysts Prepared by Two Different Methods and Their Catalytic Activity Towards the ATR of Methane. *Chem. Eng. Res. Des.* **2015**, *93*, 269−277.
(40) Hua, B.; Li, M.; Zhang, W.; Pu, J.; Chi, B.; Jian, L. Methane On-Cell Reforming by Alloys Reduced from $Ni_{0.5}Cu_{0.5}Fe_2O_4$ for Direct-Hydrocarbon Solid Oxide Fuel Cells. *J. Electrochem. Soc.* **2014**, *161*, 569−575.
(41) Vizcaíno, A. J.; Carrero, A.; Calles, J. A. Hydrogen Production by Ethanol Steam Reforming over Cu−Ni Supported Catalysts. *Int. J. Hydrogen Energy* **2007**, *32*, 1450−1461.
(42) Tavares, M. T.; Alstrup, I.; Bernardo, C. A.; Rostrup-Nielsen, J. R. Carbon Formation and CO Methanation on Silica-supported Nickel and Nickel−Copper Catalysts in CO + H_2 Mixtures. *J. Catal.* **1996**, *158*, 402−410.
(43) Chen, H. W.; Wang, C. Y.; Yu, C. H.; Tseng, L. T.; Liao, P. H. Carbon Dioxide Reforming of Methane Reaction Catalyzed by Stable Nickel Copper Catalysts. *Catal. Today* **2004**, *97*, 173−180.
(44) Fan, C.; Zhou, X. G.; Chen, D.; Cheng, H. Y.; Zhu, Y. A. Toward CH_4 Dissociation and C Diffusion during Ni/Fe-catalyzed Carbon Nanofiber Growth: A Density Functional Theory Study. *J. Chem. Phys.* **2011**, *134*, 134704−1−134704−12.
(45) Simonetti, S.; Brizuela, G.; Juan, A. Study of the Adsorption, Electronic Structure and Bonding of C_2H_4 on the FeNi(111) Surface. *Appl. Surf. Sci.* **2010**, *256*, 6459−6465.
(46) Benrabaa, R.; Boukhlouf, H.; Löfberg, A.; Rubbens, A.; Vannierb, R. N.; Bordes-Richardb, E.; Barama, A. Nickel Ferrite Spinel as Catalyst Precursor in the Dry Reforming of Methane: Synthesis, Characterization and Catalytic Properties. *J. Nat. Gas Chem.* **2012**, *21*, 595−604.
(47) Lee, J. H.; Lee, E. G.; Joo, O. S.; Jung, K. D. Stabilization of Ni/Al_2O_3 Catalyst by Cu Addition for CO_2 Reforming of Methane. *Appl. Catal. A: Gen.* **2004**, *269*, 1−6.
(48) Mizushima, T.; Tohji, K.; Udagawa, Y.; Harada, M.; Ishikawa, M.; Ueno, A. Characterization of Silica-supported Bimetallic Iron-nickel Catalysts by EXAFS. *J. Catal.* **1988**, *112*, 282−289.
(49) Lua, A. C.; Wang, H. Y. Decomposition of Methane over Unsupported Porous Nickel and Alloy Catalyst. *Appl. Catal. B: Environ.* **2013**, *132*, 469−478.
(50) Tavares, M. T.; Alstrup, I.; Bernardo, C. A. Coking and Decoking during Methanation and Methane Decomposition on Ni-Cu Supported Catalysts. *Mater. Corros.* **1999**, *50*, 681−685.
(51) La Rosa, D.; Faro, M. L.; Monforte, G.; Antonuccia, V.; Aricòa, A. S.; Sinb, A. Recent Advances on the Development of NiCu Alloy Catalysts for IT-SOFCs. *ECS Trans.* **2007**, *7*, 1685−1693.
(52) Kitla, A.; Safonova, O. V.; Föttinger, K. Infrared Studies on Bimetallic Copper/Nickel Catalysts Supported on Zirconia and Ceria/Zirconia. *Catal. Lett.* **2013**, *143*, 517−530.
(53) Popova, N. M.; Salakhova, R. K.; Dosumov, K.; Tungatarova, S. A.; Sass, A. S.; Zheksenbaeva, Z. T.; Komashko, L. V.; Grigor'eva, V. P.; Shapovalov, A. A Nickel-copper-chromium Catalyst for Selective Methane Oxidation to Synthesis Gas at Short Residence Times. *Kinet. Catal.* **2009**, *50*, 567−576.
(54) San-José-Alonso, D.; Juan-Juan, J.; Illán-Gómez, M. J.; Román-Martínez, M. C. Ni, Co and Bimetallic Ni−Co Catalysts for the Dry Reforming of Methane. *Appl. Catal. A: Gen.* **2009**, *371*, 54−59.
(55) Chen, L.; Zhu, Q.; Wu, R. Effect of Co−Ni Ratio on the Activity and Stability of Co−Ni Bimetallic Aerogel Catalyst for Methane Oxy-CO_2 Reforming. *Int. J. Hydrogen Energy* **2011**, *36*, 2128−2136.
(56) Zhang, J.; Wang, H.; Dalai, A. K. Development of Stable Bimetallic Catalysts for Carbon Dioxide Reforming of Methane. *J. Catal.* **2007**, *249*, 300−310.
(57) Yan, J. M.; Zhang, X. B.; Han, S.; Xu, Q. Magnetically Recyclable Fe−Ni Alloy Catalyzed Dehydrogenation of Ammonia Borane in Aqueous Solution under Ambient Atmosphere. *J. Power Sources.* **2009**, *194*, 478−481.
(58) Lü, Y. J.; Chen, M.; Yang, H.; Yu, D. Q. Nucleation of Ni−Fe Alloy near the Spinodal. *Acta. Mater.* **2008**, *56*, 4022−4027.
(59) Liu, H.; Wang, B.; Fan, M.; Henson, N.; Zhang, Y.; Towler, B. F. Study on Carbon Deposition Associated with Catalytic CH_4 Reforming by Using Density Functional Theory. *Fuel* **2013**, *113*, 712−718.
(60) Bernardo, C. A.; Alstrup, I.; Rostrup-Nielsen, J. R. Carbon Deposition and Methane Steam Reforming on Silica-supported NiCu Catalysts. *J. Catal.* **1985**, *96*, 517−534.
(61) Wang, Q.; Yao, J.; Rong, J.; Huang, M.; Yuan, C. Structure and Catalytic Properties of Cu-Ni Bimetallic Catalysts for Hydrogenation. *Catal. Lett.* **1990**, *4*, 63−74.
(62) Naghash, A. R.; Etsell, T. H.; Xu, S. XRD and XPS study of Cu-Ni Interactions on Reduced Copper-nickel-aluminum Oxide Solid Solution Catalysts. *Chem. Mater.* **2006**, *18*, 2480−2488.
(63) Kresse, G.; Furthmüller, J. Efficient Iterative Schemes for Ab Initio Total-Energy Calculations Using a Plane-Wave Basis Set. *Phys. Rev. B* **1996**, *54*, 11169−11186.
(64) Kresse, G.; Furthmüller, J. Efficiency of Ab-Initio Total Energy Calculations for Metals and Semiconductors Using a Plane-Wave Basis Set. *Comput. Mater. Sci.* **1996**, *6*, 15−50.
(65) White, J. A.; Bird, D. M. Implementation of Gradient-Corrected Exchange-Correlation Potentials in Car-Parrinello Total-Energy Calculations. *Phys. Rev. B* **1994**, *50*, 4954−4957.
(66) Blochl, P. E. Projector Augmented-Wave Method. *Phys. Rev. B* **1994**, *50*, 17953−17979.
(67) Perdew, J. P.; Burke, K.; Ernzerhof, M. Generalized Gradient Approximation Made Simple. *Phys. Rev. Lett.* **1996**, *77*, 3865−3868.
(68) Sheppard, D.; Xiao, P.; Chemelewski, P.; Johnson, D. D.; Henkelman, G. Generalized Solid-State Nudged Elastic Band Method. *J. Chem. Phys.* **2012**, *136*, 074103−1−074103−08.

DOI: 10.1021/acs.jpcc.5b03868
J. Phys. Chem. C 2015, 119, 14135−14144

(69) Henkelman, G.; Jónsson, H. A Dimer Method for Finding Saddle Points on High Dimensional Potential Surfaces Using Only First Derivatives. *J. Chem. Phys.* **1999**, *111*, 7010−7022.
(70) Olsen, R. A.; Kroes, G. J.; Henkelman, G.; Jónsson, H. Comparison of Methods for Finding Saddle Points without Knowledge of the Final States. *J. Chem. Phys.* **2004**, *121*, 9776−9792.
(71) Zhu, Y. A.; Chen, D.; Zhou, X. G.; Yuan, W. K. DFT Studies of Dry Reforming of Methane on Ni Catalyst. *Catal. Today* **2009**, *148*, 260−267.
(72) Wang, S. G.; Cao, D. B.; Li, Y. W.; Wang, J.; Jiao, H. Reactivity of Surface OH in CH_4 Reforming Reactions on Ni(111): A Density Functional Theory Calculation. *Surf. Sci.* **2009**, *603*, 2600−2606.
(73) Guo, X.; Liu, H.; Wang, B.; Wang, Q.; Zhang, R. Insight into C + O(OH) Reaction for Carbon Elimination on Different Types of CoNi(111) Surfaces: A DFT Study. *RSC Adv.* **2015**, *5*, 19970−19982.
(74) Fan, C.; Zhu, Y.; Zhou, X. Density Functional Theory Study of Methane Dehydrogenation on Ni-based Bimetallic Surfaces. *Chem. React. Eng. Technol.* **2012**, *28*, 117−121.
(75) Liu, H.; Zhang, R.; Yan, R.; Li, J.; Wang, B.; Xie, K. Insight Into CH_4 Dissociation on NiCu catalyst: A First-principles Study. *Appl. Surf. Sci.* **2012**, *258*, 8177−8184.
(76) Liu, H.; Zhang, R.; Ding, F.; Yan, R.; Wang, B.; Xie, K. A First-principles Study of C + O Reaction on NiCo(111) Surface. *Appl. Surf. Sci.* **2011**, *257*, 9455−9460.
(77) Liu, C.; Ye, J.; Jiang, J.; Pan, Y. Progresses in the Preparation of Coke Resistant Ni-based Catalyst for Steam and CO_2 Reforming of Methane. *ChemCatChem.* **2011**, *3*, 529−541.

DOI: 10.1021/acs.jpcc.5b03868
J. Phys. Chem. C 2015, 119, 14135−14144